

STUDY OF WATER HEATED FLOOR SYSTEM WITH SOLAR COLLECTOR

Khamraev S.I

(PhD., dosent).

Karshi Engineering Economics Institute, 180100, Karshi, Uzbekistan

ORCID ID 0000-0002-0847-9488 E-mail : xamrayev@bk.ru

Abstract

The article analyzes the energy consumption for heating a one-story model experimental house, hot water warm floor for experimentation operating at the landfill of alternative energy sources of the Karshi Institute of Engineering and Economics in Kashkadarya region. Based on the analysis, a scheme of the experimental house was created, which will be used in the development of energy saving measures for heating the buildings.

Key words

floor, heating, ventilation, indoor air temperature, outside temperature, electricity consumption, natural gas, energy saving. fuel energy, warm floor

Description of the experimental device and methodology of conducting the experiment. Currently, increasing the energy efficiency of residential houses in rural areas far from centralized energy supply and saving traditional fuel energy resources is an urgent issue [1, 2]. Especially in the winter season, it is necessary to provide heating and fuel to rural houses. One of the main ways to solve this problem is the use of renewable energy sources [3, 4, 5, 6], efficient indoor heat storage [7, 8], the use of water warm floor systems [9,10,23-27].

In recent years, water-based underfloor heating systems have been widely used in the construction of one-story houses. Previously, these systems were used as an auxiliary to the main heating system to create comfortable conditions in the rooms. The main advantage of this system is the uniform distribution of hot air inside the room. In this case, the air temperature at the foot level is 3-5 °C higher than the temperature at the head level. This temperature distribution is the most optimal for the human body [11]. Compared to the traditional heating system using radiators, the speed of convective processes is low due to the low temperature between the heating surface and the air, which leads to a decrease in air flow speeds, a decrease in the volume of exchangeable impurities and an increase in the humidity of the air in the room [12].

According to the type of heat source, underfloor heating systems are divided into two main types: electric and water. Compared to both systems, electric systems are faster to install and easier to install, but the electricity bill is significantly higher than running a water system [13]. Also, when the electric floor works, an electromagnetic field is generated, which has a harmful effect on the human body. According to [14], the maximum temperature of the floor surface in living rooms should not exceed 26°C. The required temperature on the surface of the floor with different coatings can be determined using the recommendations in [15].

At the "Alternative Energy Sources" educational and scientific site of the Karshi Institute of Engineering and Economics, a one-story experimental rural house with energy supply covered entirely by solar energy was developed and researched a water-heated floor system with a solar collector [16]. A view of the experimental house and the installed water heated floor is shown in Figure 1.1.

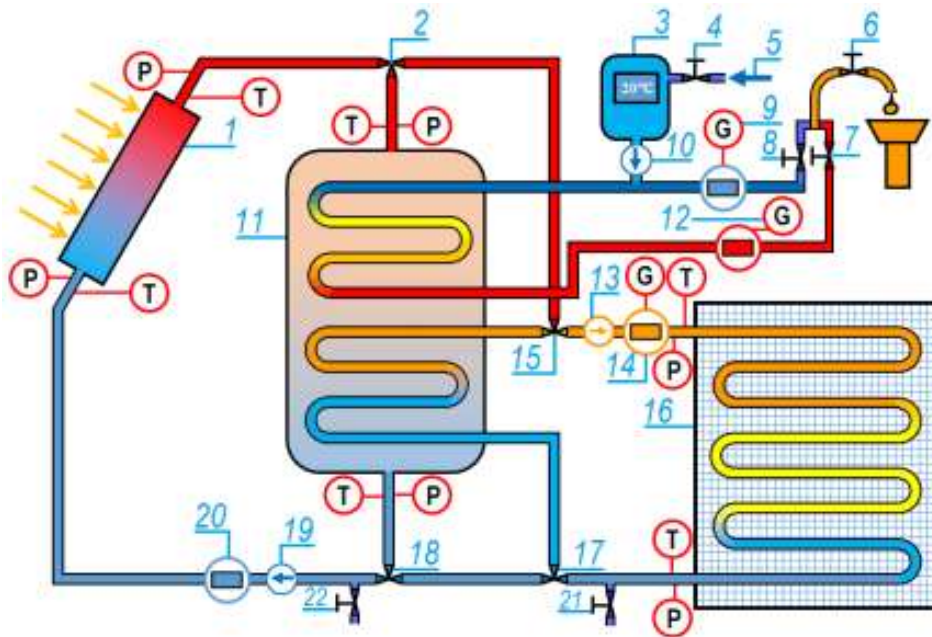


Figure 1.1. An overview of the experiment solar house and water heated floor system.

The main element of the system, the basic scheme of the water-heated floor with a solar collector, is shown in Fig. 1.2. The proposed solar collector warm floor system is designed for researching the underfloor heating system of rooms using direct solar energy, conducting experimental research on the hydrodynamic and heat exchange processes of the water warm floor system, the optimal parameters of the diameter and placement step of the warm floor pipe.

The water-heated floor system with a solar collector consists of the following main and auxiliary equipment:

a) flat solar collector - designed for heating water for a warm floor system and a tank-accumulator, and consists of the following elements: body, water moving pipe, transparent coating, heat insulating material, for measuring the temperature, pressure and consumption of water at the entrance and exit of the device control and measuring devices. The structural parameters of the flat solar collector are as follows: the total number of collectors - 5, the size of one collector - 0.7x1 m



1-solar collector; 2, 15, 17, 18 three-way valves; 3-cold water tank; 4, 6, 7, 8 valves; 5- transfer of cold water; 9, 12, 14, 20 consumption meters; 10, 13, 19-circulation pumps; 11-tank-accumulator; 16-warm floor system; Filling and draining the circuit 21, 22 with water.

Figure 1.2. The principle diagram of a warm floor system with a solar collector

b) tank-accumulator - designed to accumulate the thermal energy received by the solar collector and transfer it to the warm floor system and hot water supply, and consists of the following elements: made of a body-galvanized cylindrical tank, external insulation coating, zmeevik pipe system, temperature and pressure measuring instruments. The structural parameters of the tank-accumulator are as follows: capacity 0.1 m³, diameter 0.36 m, height 1 m, diameter of the internal zmeevik pipe 0.02 m, insulating material - foam polystyrene with a thickness of 20 mm;

c) warm floor - designed for heating the rooms from the floor, the system is created on the basis of serpentine arrangement of metal-polyethylene pipes. The diameter of the pipe is 16x2 mm, the placement step is 100 mm, 150 mm, 200 mm, 250 mm, 300 mm. The length of the pipeline varies from 32 m to 83 m, depending on the step of laying the pipeline.

The water-heated floor system with solar collectors consists of four circuits:

Circuit I - after the circuit is filled with water, the valve 18 is opened and the circulation pump 19 is started. The water supplied from the tank-accumulator passes through the consumption meter 20 and is introduced into the flat solar

collector 1, where it is heated to the required temperature due to solar energy. Then the valve 2 is opened and hot water is introduced into the tank-accumulator 11, the continuity of this process is ensured by the circulation pump. The parameters of control-measuring devices for measuring temperature and pressure are recorded on the contour;

Circuit II - after the circuit is filled with water, valves 2, 15, 17 and 18 are opened and circulation pump 19 is started. Water passes through the consumption meter 20 and is introduced into the solar collector 1, where it is heated to the required temperature due to solar energy. Then, through the valve 2 and flow meter 14 (where the circulation pump 13 is not in working condition), it is introduced into the pipe system 16 of the warm floor, where it cools down by transferring its heat to the floor and returns to the solar collector, this process continues continuously until the required temperature is provided on the floor. The parameters of control-measuring devices for measuring temperature and pressure are recorded in the outline;

Circuit III - after the circuit is filled with water, the valves 15 and 17 are opened and the water heated in the tank-accumulator 11 is introduced into the piping system of the warm floor through the consumption meter 14 with the help of the circulation pump 13. There, the water cools by transferring its heat to the floor and returns to the tank-accumulator, this process continues continuously until the required temperature is provided on the floor. The parameters of control-measuring devices for measuring temperature and pressure are recorded in the outline;

IV circuit - the necessary water reserve is collected in the cold water tank, the pump 10 is started and the flow of cold water is divided into two parts, the first part is sent directly to the water consumer, and the second part is transferred to the tank-accumulator 11 for heating. Cold and hot water passes through consumption meters 9 and 12, according to the demand of the consumer, valves 7 and 8 are opened to create the required temperature level and the consumer is supplied with hot water.

Temperature changes at the entrance and exit of hot water to the warm floor system and along the length of the pipe are measured using the KSP-4 control-measuring device. Temperatures in all other nodes are measured using thermoelectric thermometer TR-100 and bimetallic thermometers A43, A48. All circuits use the LK-20 X(G) bucket meter to measure the consumption of hot and cold water. A Testo 512 digital differential manometer is used to measure the pressure difference in all nodes.

Methodology of experimental research. In this chapter of the dissertation, experimental studies on determining the hydraulic resistance and heat transfer in the warm floor system are carried out according to the scheme presented in Figure 1.2. Experimental determination of hydraulic resistance and heat transfer coefficients in laminar and turbulent flow regimes of water in a warm floor pipeline is carried out according to the known methodology presented in [17].

To conduct experiments, the warm floor system is filled with water by opening valve 21, valves 15 and 17 are opened, then the following points are performed:

1) water is heated to the required temperature in the tank-accumulator or solar collector, then the circulation pump 13 is started and water passes through the consumption meter 14. The consumption of hot water delivered to the working section is adjusted using valves 17 and 15;

2) the flow mode of hot water is provided depending on the studied mode, then the specified speed and water consumption are set. In the pipe system of the warm floor, hot water is circulated for 5 minutes, after the end of the circulation, the specified consumption of hot water is set, and this consumption and mode is strictly maintained for 5 minutes, then the pressure loss is measured using a manometer and the temperatures of water at the inlet and outlet are measured using a thermometer. The measurement of temperature and pressure loss for each mode is done in this way;

3) turning off the experimental device is carried out in the following order: the circulation pump 13 is disconnected from the electrical network. When valves 15 and 17 are open, valve 21 is opened and the system is emptied of water. After the system is emptied, valves 15, 17 and 21 are closed. This concludes the experiment.

Experimental study of the hydrodynamic regime of a solar collector water heated floor system. An experimental study of the hydrodynamic mode of the warm floor pipe was carried out according to the scheme shown in Figure 1.6. Experimental studies were carried out in the following range of main parameters: consumption of hot water: in laminar flow mode $G=0,0043\div 0,02$ kg/sec, in the turbulent flow regime $G=0,07\div 0,093$ kg/sec; average hot water temperature $t_c = 35 \dots 50^\circ\text{C}$; average temperature on the floor surface $t_{floor} = 26^\circ\text{C}$; the diameter of the pipe $d = 0,016$ m; pipe placement step $s = 0,1$ m, $s = 0,15$ m, $s = 0,2$ m, $s = 0,25$ m, $s = 0,3$ m; the speed of hot water in the underfloor heating pipe should not exceed 1 m/sec [18].

To determine the area of the laminar flow regime, it is necessary to calculate the value of the product $Gr \cdot Pr$ [19]:

$$Gr \cdot Pr = g\beta_r \frac{\Delta t d^3}{\nu_r^2} Pr_r \quad (1.1)$$

where Gr-Grasof number; Pr-Prandtl number; g-acceleration of free fall, m/s²; β -coefficient of volume expansion, 1/°C; Δt -temperature difference, °C; d-pipe inner diameter, m; ν -kinematic viscosity coefficient, m/s²; index " r " indicates that the physical properties of liquids are obtained by temperature $t_r = 0,5(t_s + t_d)$.

When $Gr \cdot Pr < 8 \cdot 10^5$, the flow regime is viscous. In the presence of heat exchange, the hydraulic resistance in smooth pipes in the viscous region of the laminar flow regime is defined as [20]:

$$\xi = \frac{64}{Re} \left(\frac{\mu_d}{\mu_c} \right)^n \quad (1.2)$$

here $n = C \left(Pe_1 \frac{d}{l} \right)^m \left(\frac{\mu_d}{\mu_c} \right)^{-0,062}$; $Pe_1 \frac{d}{l} = \frac{4G c_p}{\pi l \lambda_c}$; $Pe_1 \frac{d}{l} \leq 1500$ when $C = 2,3$; $m = -0,3$; $Pe_1 \frac{d}{l} \geq 1500$ when $C = 0,535$; $m = -0,1$ Re- Reynolds number.

When $Gr \cdot Pr > 8 \cdot 10^5$ the flow regime is viscous-gravitational. In the presence of heat exchange, the hydraulic resistance in smooth pipes in the viscous-gravitational field of the laminar flow regime is determined as follows [124]:

$$\xi = \frac{64}{Re} \left(\frac{Pr_d}{Pr_s} \right)^{1/3} \left[1 + 0,22 \left(\frac{GrPr}{Re} \right)^{0,15} \right] \quad (1.3)$$

In the presence of heat exchange, the hydraulic resistance in the turbulent flow regime is defined as [21]:

$$\xi = \frac{0,3164}{Re^{0,25}} \left(\frac{Pr_d}{Pr_s} \right)^{1/3} \quad (1.4)$$

The total pressure loss in a water-heated floor node is equal to the sum of the linear pressure loss and the pressure loss overcoming local resistances [21]:

$$\Delta p_y = \Delta p_q + \Delta p_m \quad (1.5)$$

Linear pressure loss in a water-heated floor pipe [21]:

$$\Delta p_q = \xi \frac{\rho w^2 d}{2 l} \quad (1.6)$$

here ρ - density of hot water, kg/m³; w- the speed of hot water in the pipe, m/s; d- inner diameter of the pipe, m; l- the total length of the pipe, m.

Pressure loss to overcome local resistances in a water-heated floor pipe [21]:

$$\Delta p_m = \sum \xi \frac{\rho w^2}{2} \quad (1.7)$$

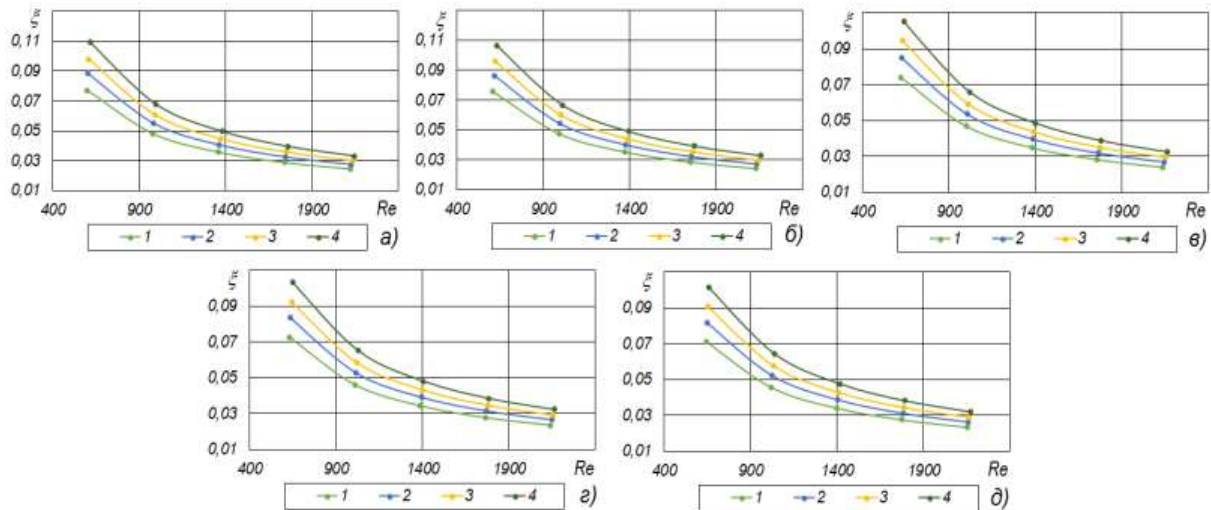
here $\sum \xi$ - sum of local (all bends ("elbow")) resistances at the node.

The pump power required to drive the hot water passing through the water warm floor pipe is determined by the following formula [21]:

$$N = \frac{G \Delta p_y}{\rho \eta} \quad (1.8)$$

here G- consumption of hot water, kg/sec; η - Pump Efficiency, usually $\eta=0,7$.

Laminar flow mode. Experimental results on the coefficient of hydraulic resistance of the pipe in the laminar flow mode of hot water at different location steps of the warm floor pipe and at different temperatures of hot water are presented in Figure 1.3, and the experimental results on pressure loss and pump power are presented.



a-s=100 mm; б-s=150 mm; B-s=200 mm; r-s=250 mm; д-s=300 mm;
1- $t_{water} = 35^{\circ}\text{C}$; 2- $t_{water} = 40^{\circ}\text{C}$; 3- $t_{water} = 45^{\circ}\text{C}$; 4- $t_{water} = 50^{\circ}\text{C}$

Figure 1.3. Graphs of changes in the coefficient of hydraulic resistance in the laminar flow mode depending on the placement step of the warm floor pipe and the hot water temperature

The analysis of the results of the hydraulic resistance coefficient presented in Figure 1.3 shows that the hydraulic resistance coefficient of the warm floor pipe is significantly dependent on the pipe layout step and the hot water temperature, and the hydraulic resistance coefficient increases as the pipe layout step decreases and the hot water temperature increases. According to the experimental results, the coefficient of hydraulic resistance is 0.024...0.109 when the positioning step is 100 mm in laminar flow mode, 0.024...0.107 when it is 150 mm, 0.024...0.105 when it is 200 mm, 0.024...0.103 when it is 250 mm, when it is 300 mm It was determined to vary between 0.024...0.101.

The experimental results obtained on hydraulic resistance in the laminar flow mode were processed and the following empirical relationships were obtained at different placement steps of the pipe:

$s = 100 \text{ mm}$ when:

$$\xi = \frac{20,967}{Re^{0,924}} \left(\frac{Pr_d}{Pr_s} \right)^{1,037} \left(\frac{GrPr}{Re} \right)^{0,012} \quad (1.9)$$

$s = 150 \text{ mm}$ when:

$$\xi = \frac{20,843}{Re^{0,926}} \left(\frac{Pr_d}{Pr_s}\right)^{1,035} \left(\frac{GrPr}{Re}\right)^{0,014} \quad (1.10)$$

$s = 200 \text{ mm}$ when:

$$\xi = \frac{21,023}{Re^{0,928}} \left(\frac{Pr_d}{Pr_c}\right)^{1,037} \left(\frac{GrPr}{Re}\right)^{0,014} \quad (1.11)$$

$s = 250 \text{ mm}$ when:

$$\xi = \frac{21,299}{Re^{0,931}} \left(\frac{Pr_d}{Pr_s}\right)^{1,040} \left(\frac{GrPr}{Re}\right)^{0,014} \quad (1.12)$$

$s = 300 \text{ mm}$ when:

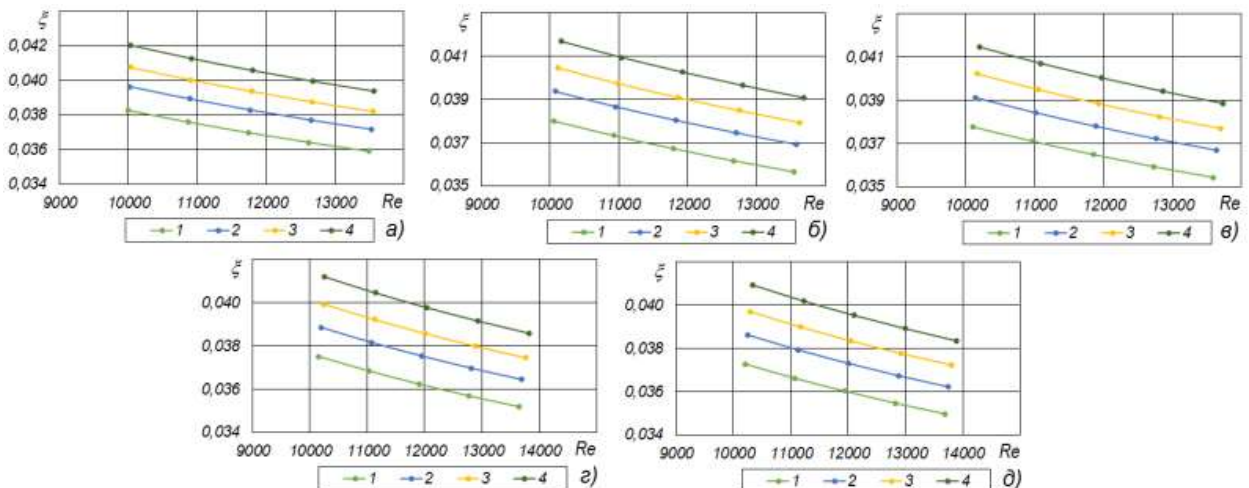
$$\xi = \frac{21,347}{Re^{0,933}} \left(\frac{Pr_d}{Pr_s}\right)^{1,040} \left(\frac{GrPr}{Re}\right)^{0,015} \quad (1.13)$$

In the generalized case, the following equation was obtained:

$$\xi = \frac{20,44}{Re^{0,929_s 0,018}} \left(\frac{Pr_d}{Pr_s}\right)^{1,038} \left(\frac{GrPr}{Re}\right)^{0,014} \quad (1.14)$$

The obtained relation (1.14). $400 < Re < 2200$, $1,25 < Pr_d / Pr_s < 1,71$, $9,7 \cdot 10^5 < GrPr < 34 \cdot 10^5$ appropriate at intervals. Calculation error $\pm 2\%$.

Turbulent flow mode. Experimental results on the coefficient of hydraulic resistance of the hot water pipe in the turbulent flow regime of the warm floor pipe at different location steps and at different hot water temperatures are shown in Figure 1.4, and the experimental results on pressure loss and pumping power are presented.



a- $s=100 \text{ mm}$; б- $s=150 \text{ mm}$; в- $s=200 \text{ mm}$; г- $s=250 \text{ mm}$; д- $s=300 \text{ mm}$;
 1- $t_{water} = 35^\circ\text{C}$; 2- $t_{water} = 40^\circ\text{C}$; 3- $t_{water} = 45^\circ\text{C}$; 4- $t_{water} = 50^\circ\text{C}$

Figure 1.4. Variation of the coefficient of hydraulic resistance in the turbulent flow regime depending on the placement step of the warm floor pipe and the temperature of the hot water

The analysis of the results of the hydraulic resistance coefficient presented in Figure 1.4 shows that the hydraulic resistance coefficient of the warm floor pipe is significantly dependent on the pipe layout step and the hot water temperature, and the hydraulic resistance coefficient increases as the pipe layout step decreases and the hot water temperature increases. According to the experimental results, the hydraulic resistance coefficient is 0.036...0.042 when the placement step is 100 mm in the turbulent flow mode, 0.035...0.41 when it is 150 mm, 0.034...0.040 when it is 200 mm, 0.033...0.039 when it is 250 mm, 300 mm, it was found to change in the range of 0.032...0.038.

The experimental results obtained on the hydraulic resistance in the turbulent flow mode were processed and the following empirical correlations were obtained at different placement steps of the pipe.:

$s = 100 \text{ mm}$ when:

$$\xi = \frac{0,258}{Re^{0,214}} \left(\frac{Pr_d}{Pr_s} \right)^{0,295} \quad (1.15)$$

$s = 150 \text{ mm}$ when:

$$\xi = \frac{0,259}{Re^{0,215}} \left(\frac{Pr_d}{Pr_s} \right)^{0,297} \quad (1.16)$$

$s = 200 \text{ mm}$ when:

$$\xi = \frac{0,26}{Re^{0,216}} \left(\frac{Pr_d}{Pr_s} \right)^{0,298} \quad (1.17)$$

$s = 250 \text{ mm}$ when:

$$\xi = \frac{0,262}{Re^{0,218}} \left(\frac{Pr_d}{Pr_s} \right)^{0,3} \quad (1.18)$$

$s = 300 \text{ mm}$ when:

$$\xi = \frac{0,263}{Re^{0,219}} \left(\frac{Pr_d}{Pr_s} \right)^{0,301} \quad (1.19)$$

In the generalized case, the following equation was obtained:

$$\xi = \frac{0,252}{Re^{0,217} s^{0,019}} \left(\frac{Pr_d}{Pr_c} \right)^{0,298} \quad (1.20)$$

Equation (1.20) derived from the above equations $10000 < Re < 14000$, $1,25 < Pr_d / Pr_s < 1,71$ appropriate at intervals. Calculation error $\pm 2\%$.

Assessment of adequacy of theoretical and experimental results of hydrodynamic research. Adequacy was assessed by Fisher's criterion [22]:

$$F_{cal} = \frac{S_{ad}^2}{S_y^2} \quad (1.21)$$

where S_{ad} - is the adequacy dispersion of the models; S_y - is the variance of mutual proximity of y quantities

Adequacy variance:

$$S_{ad}^2 = \frac{\sum_{i=1}^n (y - \hat{y})^2}{f_1} \quad (1.22)$$

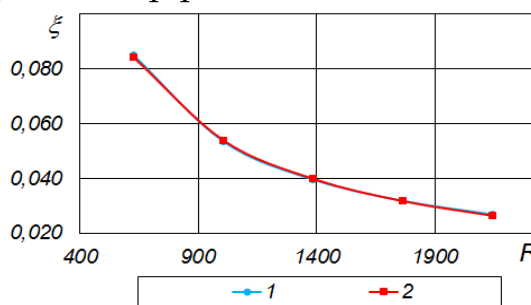
where y - is a theoretical function; \hat{y} - is the desired function; f_1 - is the number of degrees of freedom.

Mutual proximity variance:

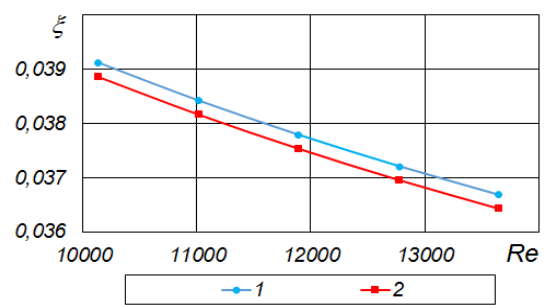
$$S_y^2 = \frac{\sum_{i=1}^n (y - \bar{y})^2}{n-1} \quad (1.23)$$

here $\bar{y} - y$ Arithmetic mean value of; n - number of observations.

Figure 1.5 shows a comparison of the theoretical and experimental results obtained for the determination of hydraulic resistance in laminar and turbulent flow regimes in a pipe.



1-theoretical (formula 1.3) results; Results of experiment 2 (formula 1.14).



1-theoretical (formula 1.4) results; Results of experiment 2 (formula 1.20).

Figure 1.5. Comparison of theoretical and experimental results obtained on hydraulic resistance in laminar and turbulent flow regimes

Confidence Probability from Table of Fisher's Criterion Values $P=0,99$, degrees of freedom $f_1 = 95$ and number of observations $n = 99$ suitable for the case $F_{table} = 0,62$ we find the value. Calculated value of the Fisher criterion for the formula (1.14). $F_{calculation} = 0,3$. Calculated value of the Fisher criterion for the formula (1.20). $F_{calculation} = 0,13$. It can be seen that in both cases $F_{cal} < F_{table}$, so the model is adequate. Empirical correlations obtained for determining the hydraulic resistance in warm floor pipes are fully adequate with the experimental results, and they can be used to evaluate the hydrodynamic efficiency of the warm floor system with solar collectors in different flow regimes of hot water.

Summary.

1. The influence of the temperature of hot water moving from the warm floor pipe and the step of the pipe placement on the coefficient of hydraulic resistance, pressure loss in the pipe and pump power was experimentally studied in laminar and turbulent flow modes of hot water. According to the experimental results,

when the hot water temperature is 35-50°C and the pipe pitch is 0.1-0.3m in the laminar flow mode, the heat transfer coefficient, the hydraulic resistance coefficient is in the range of 0.024-0.109, the pressure loss is in the range of 55-612 Pa, and the pump power is 1- It was found to vary in the range of 17 W. In the turbulent flow mode, when the temperature of hot water is 35-50°C and the pitch of the pipe is 0.1-0.3 m, the coefficient of hydraulic resistance is in the range of 0.032-0.042, the pressure loss is in the range of 5506-36733 Pa, and the pump power is found to vary in the range of 6-65 W.

2. The influence of hot water temperature moving from the pipe of the warm floor pipe and the step of placement of the pipe on the heat transfer coefficient, convective heat exchange and the amount of transferred heat was experimentally studied. According to the results of the experiment, it was determined that the coefficient of heat transfer in the laminar flow mode is in the range of 0.82-2.35, the convective heat transfer is in the range of 33-92 W/(m²·°C), the amount of transferred heat is in the range of 835-5438 W. It was determined that the coefficient of heat transfer in the turbulent flow regime is in the range of 49-78, convective heat transfer is in the range of 1973-3089 W/(m² ·°C), the amount of transferred heat is in the range of 52883-251348 W.

REFERENCES

1. K. Yu, Y. Tan, T. Zhang, J. Zhang, X. Wang, The traditional Chinese kang and its improvement: A review, *Energy Build.* 218 (2020) 110051, <https://doi.org/10.1016/j.enbuild.2020.110051>.
2. Z. Zhuang, Y. Li, B. Chen, J. Guo, Chinese kang as a domestic heating system in rural northern China-A review, *Energy Build.* 41 (1) (2009) 111-119.
3. D. Wang, R. Zhang, Y. Liu, X. Zhang, J. Fan, Optimization of the flow resistance characteristics of the direct return flat plate solar collector field, *Sol. Energy* 215 (2021) 388-402.
4. S. Paraschiv, N. B̂arbuȚȃ-MisȚu, L.S. Paraschiv, Technical and economic analysis of a solar air heating system integration in a residential building wall to increase energy efficiency by solar heat gain and thermal insulation, *Energy Reports*, S 6 (2020) 459-474.
5. H. Esen, M. Esen, O. Ozsolak, Modelling and experimental performance analysis of solar-assisted ground source heat pump system, *J. Exp. Theor. Artif. Intell.* 29 (1) (2017) 1-17.

6. Uzakov G.N., Khamraev S.I., Khuzhakulov S.M. Rural house heat supply system based on solar energy // IOP Conf. Series: Materials Science and Engineering 1030 (2021) 012167 IOP Publishing doi:10.1088/1757-899X/1030/1/012167.
7. M. Esen, T. Ayhan, Development of a model compatible with solar assisted cylindrical energy storage tank and variation of stored energy with time for different phase change materials, Energy Convers. Manage 37 (12) (1996) 1775–1785.
8. M. Esen, A. DurmusЯ, A. DurmusЯ, Geometric design of solar-aided latent heat store depending on various parameters and phase change materials, Sol.Energy 62 (1998) 19–28.
9. Y. Liu, T. Li, C. Song, D. Wang, J. Liu, Field study of different thermal requirements based on the indoor activities patterns of rural residents in winter in Northwest China, Science and Technology for the, Built Environment 24 (8) (2018) 867–877.
10. Y.Y. Wang, W.J. Kang, Y.F. Liu, R. Huang, J.P. Liu, A heating strategy for rural residential buildings based on behavior patterns of residents in shaanxi province, Acta energiae solaris sinica 39 (2018) 3026–3031 (In chinese).
11. Низовцев М.И., Сахаров И.А. Определение тепловых и конструктивных параметров водяного теплого пола // Научно-практическая конференция “Энерго-и ресурсоэффективность малотэтажных жилых зданий”. Институт теплофизики С.С. Кутателадзе СО РАН, 19-20 марта 2013 г. – с. 39-42.
12. Bearzi V. Теплые полы. Теория и практика // АВОК. – 2005. №7. – с. 70-82.
13. Почему водяной теплый пол, а не электрический. ООО «ВАНТУБО-СЕРВИС» [Электронный ресурс] URL: <http://www.vantubo-service.ru/neelectro>.
14. СНиП 41-01-2003. «Отопление, вентиляции и кондиционирование».
15. ГОСТ 13732-2-2008. «Эргономика термальной среды. Методы оценки реакции человека при контакте с поверхностями. Часть2. Контакт с поверхностью умеренной температуры».
16. Хамраев С.И., Хужакулов С.М., Камолов Б.И. Қуёш иссиқлик таъминоти тизимли тажриба қишлоқ уйининг иссиқлик балансини тадқиқот қилиш. // «Энергия ва ресурс тежаш муаммолари». Тошкент, 2021. № 3, 181-191-б.

17. Руководство к практическим занятиям в лаборатории процессов и аппаратов химической технологии: Учебное пособие для вузов. / Под ред. П.Г. Романкова. – Л.: Химия, 1990. – 272 с.
18. Водяной теплый пол. Проектирование, монтаж, настройка. 2020. www.valtek.ru.
19. Краснащекоев Е.А., Сукомел А.С. Задачник по теплопередаче: Учебное пособие для вузов. – М.: Энергия, 1980. – 288 с.
20. Каневец Г.Е. Обобщенные методы расчета теплообменников. – Киев: Наук, думка, 1979, - 352 с.
21. Михеев М.А., Михеева И.М. Основы теплопередачи. Изд. 2-е. М.: Энергия, 1977. – 344 с.
22. Бабин А.В., Ракипов Д.В. Организация и математическое планирование эксперимента. Екатеринбург, уральский Федеральный Университет, 2014. – 113 с.
23. [L. A. Aliyarova](#), [U. H. Ibragimov](#), [S. I. Khamraev](#). Investigation of hydrodynamic processes in tubes of a combined solar collector. AIP Conference Proceedings 2612, 030018 (2023); <https://doi.org/10.1063/5.0124758>
24. Uzakov G. N., Charvinski V. L., Ibragimov U. Kh., Khamraev S. I., Kamolov B. I. (2022) Mathematical Modeling of the Combined Heat Supply System of a Solar House. Energetika. Proc. CIS Higher Educ. Inst. and Power Eng. Assoc. 65 (5), 412–421. <https://doi.org/10.21122/1029-7448-2022-65-5-412-421>
25. Sh Mirzaev, J Kodirov, S I Khamraev. Method for determining the sizes of structural elements and semi-empirical formula of thermal characteristics of solar dryers// APEC-V-2022 IOP Conf. Series: Earth and Environmental Science IOP Conf. Series: Earth and Environmental Science 1070(2022) 012021 IOP Publishing doi:10.1088/1755-1315/1070/1/012021.
26. S I Khamraev. Study of the combined solar heating system of residential houses. BIO Web of Conferences 71, 02017 (2023) <https://doi.org/10.1051/bioconf/20237102017> CIBTA-II-2023
27. [Saydullo Khuzhakulov](#), [Zokir Pardaev](#), [Sardor Khamraev](#). Thermal conditions of systems for solar thermal regeneration of adsorbents // IPICSE 2020 IOP Conf. Series: Materials Science and Engineering 1030 (2021) 012166 IOP Publishing doi:10.1088/1757-899X/1030/1/012166